GEOLOGIJA *65/1*, 101–121, Ljubljana 2022

https://doi.org/10.5474/geologija.2022.007

Multi-method study of the Roman quarry at Podpeč sedimentary succession and stone products

Večmetodne raziskave sedimentarnega zaporedja in kamnitih izdelkov rimskodobnega kamnoloma v Podpeči

Rok BRAJKOVIČ[1], Luka GALE[1,2] & Bojan DJURIĆ[3]

[1]Geological Survey of Slovenia, Dimičeva ul. 14, SI-1000 Ljubljana, Slovenia; e-mail: rok.brajkovic@geo-zs.si; luka.gale@geo-zs.si
[2]Faculty of Natural Sciences and Engineering, Department of Geology, Aškerčeva 12, SI- 1000 Ljubljana, Slovenia; e-mail: luka.gale@ntf.uni-lj.si
[3]Faculty of Arts, Department of Archaeology, Aškerčeva 2, SI-1000 Ljubljana, Slovenia; e-mail: bojan.djuric@gmail.com

Prejeto / Received 7. 3. 2022; Sprejeto / Accepted 15. 7. 2022; Objavljeno na spletu / Published online 22. 07. 2022

Key words: Lower Jurassic, Podbukovje Formation, provenance, facies, foraminifera, geochemistry, Emona, geoarchaeology
Ključne besede: spodnja jura, Podbukovška formacija, provenienca, facies, foraminifere, geokemija, Emona, geoarheologija

Abstract

The paper presents a multi-method characterisation of the Roman quarry of the middle Lower Jurassic (Pliensbachian) limestone situated in the village of Podpeč, south of Ljubljana, and examples of the placement of stone products made from micritic, fine-grained, and oolithic facies into the known extent of the quarry. 23 m of the rock succession from the ancient quarry was exposed at the northern tip of the St. Ana Hill by archaeological trenching. Petrological, micropaleontological, mineralogical, geochemical, and isotopic analyses of carbon, oxygen, and strontium were performed in order to characterise the rocks exploited in the quarry. Additionally, a new detailed geological map of the wider Podpeč area was prepared, which defines in detail the lithostratigraphic units in the area.

The recorded succession contains facies that also occur in the modern part of the quarry. Interpretation of the sedimentation environment is consistent with previous interpretations and occurred in an internally differentiated lagoon. The studied succession is characterised by $\delta^{13}C$ isotope values ranging from -2.44 to +2.5 ‰; $\delta^{18}O$ values ranging from -4.0 to -1.2 ‰; and $^{87}Sr/^{86}Sr$ values ranging from 0.707414 ‰ (SD 0.000003) to 0.707329 ‰ (SD 0.000012). The Sr isotope values can prove a decisive factor when studying the provenance of stone products, while $\delta^{13}C$ and $\delta^{18}O$ values can help narrow the place of extraction within the known extent of the Roman quarry at Podpeč. The high positive correlation of SiO_2 with Al_2O_3, K_2O and TiO_2 recognised both in the logged succession and in the studied stone products indicates a low terrigenous input into the depositional area and further confirms the provenance determination.

By applying a multi-method approach to the characterisation of the known extent of the ancient part of the Podpeč quarry, we have reliably determined the provenance of stone products that have their origin in the quarry and have successfully applied this approach to several stone products made of micritic, fine-grained and oolithic limestones.

Izvleček

Članek predstavlja večmetodno karakterizacijo rimskega kamnoloma v vasi Podpeč južno od Ljubljane in primere umeščanja apnenca kamnitih izdelkov iz spodnjejurskih (pliensbachijskih) mikritnih, drobnozrnatih in oolitnih faciesov v znan obseg kamnoloma. Na severnem robu hriba sv. Ane je bilo z arheološkimi izkopi razkrito 23 m debelo kamninsko zaporedje antičnega kamnoloma. Za karakterizacijo kamnin, ki so jih izkoriščali v kamnolomu, so bile opravljene petrološke, mineraloške, mikropaleontološke in geokemične analize ter izotopske analize ogljika, kisika in stroncija. Poleg tega je bila izdelana nova podrobna geološka karta širšega območja Podpeči, na kateri so natančno opredeljene litostratigrafske enote na tem območju.

Preučeno zaporedje vsebuje faciese, ki se pojavljajo tudi v sodobnem delu kamnoloma. Potrjena je bila interpretacija sedimentacije v notranje diferencirani laguni. Za preučeno zaporedje so značilne vrednosti izotopov $\delta^{13}C$ od -2,44 do +2,5 ‰, vrednosti $\delta^{18}O$ od -4,0 do -1,2 ‰ in vrednosti $^{87}Sr/^{86}Sr$ od 0,707414 ‰

(SD 0,000003) do 0,707329 ‰ (SD 0,000012). Izotopske vrednosti Sr lahko uporabimo kot najzanesljivejši podatek pri določitvi izvora kamnitih izdelkov, vrednosti $\delta^{13}C$, $\delta^{18}O$ pa lahko pomagajo pri zožitvi opredelitve mesta pridobivanja znotraj znanega zaporedja plasti rimskega kamnoloma v Podpeči. Visoka pozitivna korelacija SiO_2 z Al_2O_3, K_2O in TiO_2, ugotovljena v preučenem zaporedju in kamnitih izdelkih, kaže na majhen vnos terigene komponente v primarno sedimentacijsko okolje ter dodatno potrjuje določitev provenience.

Z uporabo večmetodnega pristopa h karakterizaciji znanega obsega antičnega dela Podpeškega kamnoloma smo omogočili zanesljivo določitev izvora kamnitih izdelkov iz kamnoloma in ta pristop uspešno uporabili na več kamnitih izdelkih izdelanih iz mikritnih, drobnozrnatih in oolitnih apnencev.

Introduction

The present article follows the publication by Djurić et al. (2022), in which the authors defined the location of the ancient quarry at Podpeč and investigated the stone products with presumed origin from the quarry. Since the provenance of micritic, fine-grained, as well as partially oolithic limestones used to produce stone products could not be reliably determined using the macro- and microscopic studies presented in previous studies, further analyses were carried out and are presented in this article. This study was prepared using a multi-method approach widely used in geoarchaeology (Galan et al., 1999; Maritan et al., 2003; Brilli et al., 2010; Brilli et al., 2011; Šmuc et al., 2016; Miletić et al., 2021).

The middle Lower Jurassic (Pliensbachian) limestone from quarries at Podpeč, south of Ljubljana, is amongst the well-known dimension stones in Slovenia (Mirtič et al., 1999; Ramovš, 2000). Among the beds of different colours and textures we also find dark grey to almost black limestone with white shells of lithiotid bivalves, which was particularly valued for its decorative properties throughout the 20th century (Ramovš, 2000). The history of quarrying in Podpeč, however, goes as far back as Antiquity (Müllner, 1879; Brodar et al., 1955; Šašel Kos, 1997; Ramovš, 2000; Kramar et al., 2015; Djurić & Rižnar, 2017; Djurić et al., 2017; Djurić et al., 2022). According to Djurić et al. (2022), a well-organised and continuous production of dimension stone can be confirmed – at least for the period between the 1st and 3rd centuries AD when the area belonged to Regio X (Italia) of the Roman state. The production of stone from this area, however, may go even further back in time to the earliest beginnings of the Roman colony (Djurić & Rižnar, 2017). Most of these stone products ended up in Emona, a colony located 15 km to the north of present-day Ljubljana, which was connected to the quarry via the Ljubljanica River (Djurić & Rižnar, 2017; Djurić et al. 2018b; Djurić et al., 2022). Based on the lithological characteristics of the limestone beds, the historical topography of the village of Podpeč, and the archaeological remains, the exact location of the Roman quarry was very likely the northern tip of the St. Ana hill (Fig. 1) (Djurić et al., 2022). The entire succession exposed in both the ancient and modern Podpeč quarry, from the base of the archaeological trenches (probes) in the north, to the base of the

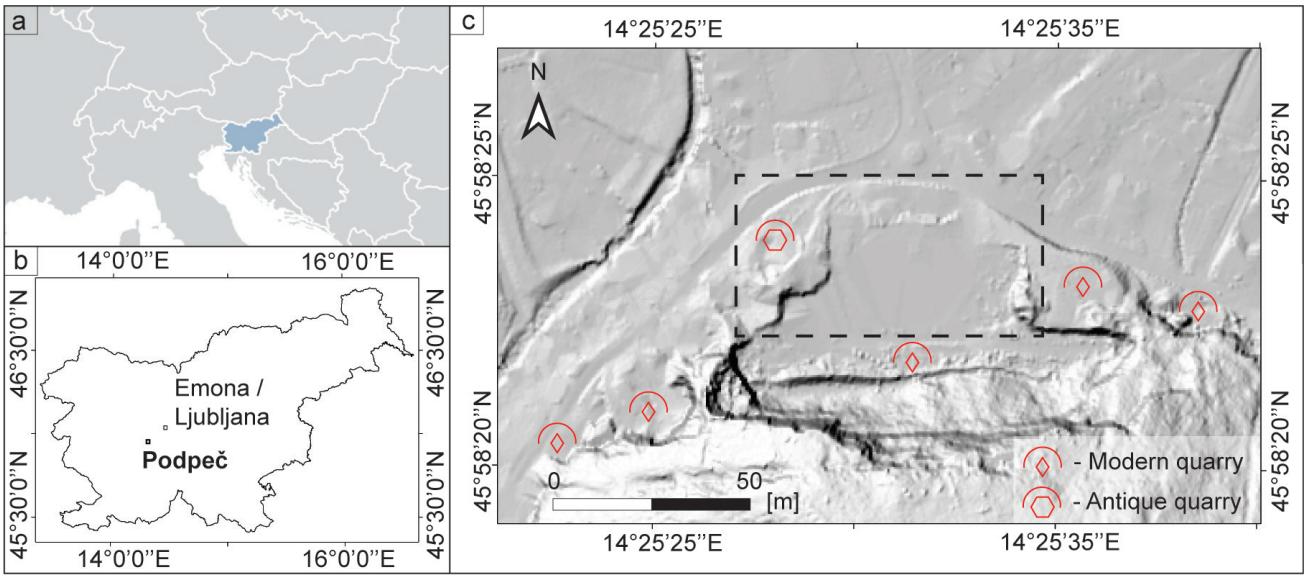

Fig. 1. Position of the main quarries at Podpeč. a: Marked position of Slovenia. b: Position of the modern village of Podpeč. c: Narrow study area at the village of Podpeč with marked position of Figure 3. The source of the topography is a 1 m × 1 m resolution digital relief model (The Surveying and Mapping Authority of the Republic of Slovenia, 2011).

Laze Formation in the south, measures 114 stratigraphic meters in thickness, and approximately 30 m of this succession is known to be quarried during the Antiquity (Djurić et al., 2022).

Covered by rubble and built upon, the surface of the antique quarry is no longer visible today. Parts of it were, however, accessible during archaeological excavations in 2016 and 2017 (Djurić et al., 2017, Djurić et al., 2022). Methodological approaches used to determine provenance can vary depending on the lithology in question, while a common denominator in the study of limestone provenance in recent decades is the multi-method approach proposed by Galan et al. (1999). This approach was recognized as the most effective and has since successfully been replicated and further developed by numerous authors (e.g. Maritan et al., 2003; Brilli et al., 2010, 2011).

Whereas the facies of the limestone beds uncovered in archaeological probes is briefly described in Djurić et al. (2022), the purpose of this paper is to provide a detailed multi-method characterisation of the beds excavated in the antique quarry and to use this data to help determine the provenance of the stone products. The hypothesis set-out held that by applying the same multi-method characterization approach to the ancient quarry and stone products samples, reliable provenance determinations of Roman stone products could also be made for micritic, fine-grained, and oolithic facies in stone products. These facies can also be found in other possible source-areas located near Emona, e.g. Podutik (Ramovš, 1990; Vodnik, 2017) or Staje (Rožič et al., 2018). Therefore, it is important for any further studies on the provenance of stone products to define their characteristics in the ancient Podpeč quarry. In addition to the detailed multi-method characterisation of the antique Podpeč quarry and stone products, a geological map of the wider research area was prepared in order to define the stratigraphic units available for quarrying and their spatial relationships in the wider Podpeč area.

Geological setting

The Podpeč quarry is situated in central Slovenia at the base of the St. Ana hill, which represents the northern tip of the mountain range overlooking the Barje basin. The range itself and the rocky base of the Quaternary Barje basin (Vrabec & Fodor, 2006) are structurally part of the External Dinarides thrust system (more precisely, of the Hrušica Nappe), mainly formed during the Oligocene-early Miocene (Placer, 1999; Vrabec & Fodor, 2006). The SW-verging Dinaric thrust units are largely composed of carbonate rocks, which deposited during the Mesozoic on the Adriatic Carbonate Platform (Vlahović et al., 2005). The rocky southern surroundings of the Podpeč quarry (Fig. 2a) are thus mostly formed of the Upper Triassic peritidal dolomite of the Main Dolomite Formation, the Lower Jurassic

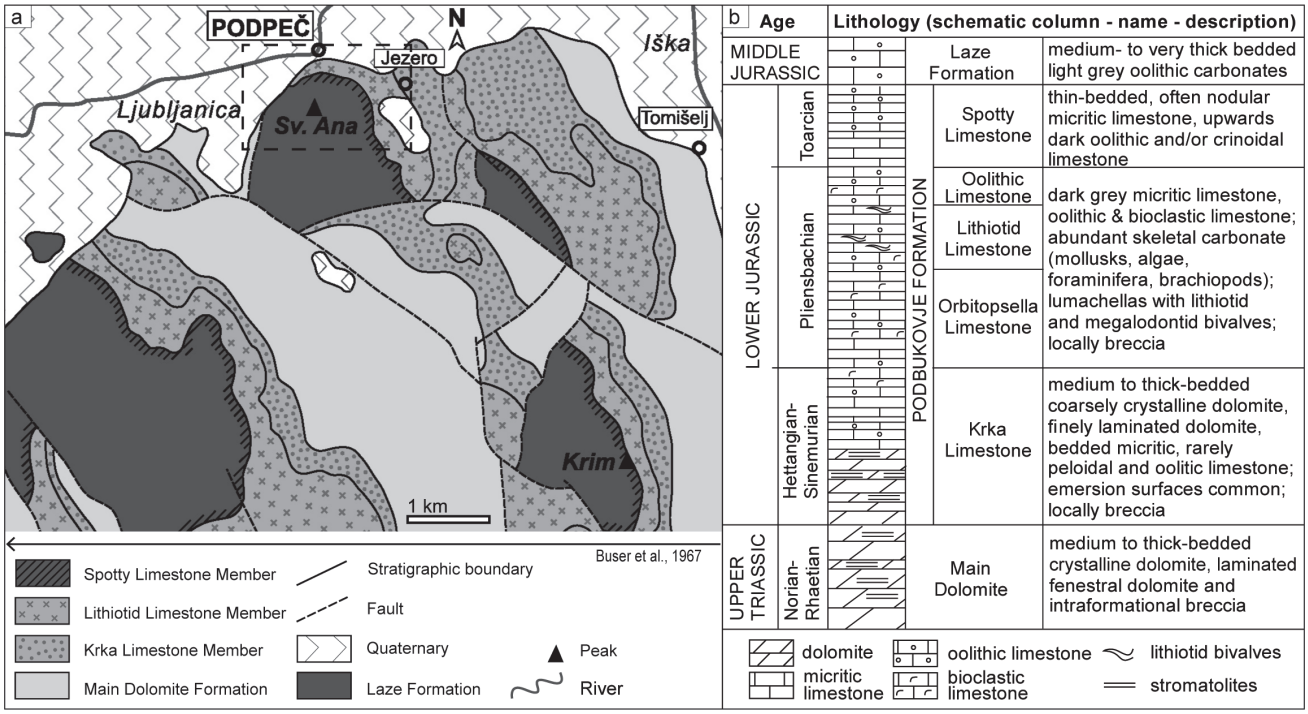

Fig. 2. Geological map of the quarry at Podpeč (modified after Buser, 1967) with stratigraphic column modified after Dozet & Strohmenger (2000) with marked area (dashed rectangle) of the broader research area.

dolomites and predominant limestones of the Podbukovje Formation, and the Middle Jurassic oolithic limestones of the Laze Formation (Fig. 2b) (Buser et al., 1967; Buser, 1968; Ogorelec & Rothe, 1993; Miler & Pavšič, 2008; Ogorelec, 2009; Gale & Kelemen, 2017). The Podbukovje Formation is further divided into five members. The lowest is the Hettangian to Sinemurian Krka Limestone Member, characterised by micritic limestone successions with signs of subaerial exposure (Dozet, 2009). The Orbitopsela Limestone Member (Orbitopsella beds) is the second member, for which Pliensbachian age was determined owing to the occurrence of large Orbitopsella foraminifera. The stratigraphic range of this genus, however, continues to the third member, known as the Lithiotid Limestone Member (Gale, 2015), characterised by Lithiotid bivalves (Buser & Debeljak, 1995; Debeljak & Buser, 1997). The fourth member is the Oolithic limestone (Dozet, 2009), still Pliensbachian in age. The Podbukovje Formation ends with the dark micritic Toarcian Spotty Limestone Member. This in turn gradually passes into the Middle Jurassic oolithic limestone of the Laze Formation (sensu Dozet & Strohmenger 2000).

Material and methods

The broader research area was geologically mapped at a scale of 1: 5000.

The lithological succession in the antique quarry in Podpeč was logged in three probes (archaeological trenches) dug in the years 2016–2017 immediately north and northwest of the modern quarry, at the northernmost base of the St. Ana hill. An additional section was logged in the basement of House Podpeč 44 (Fig. 3). Based on these partial sections, a composite section 23 m thick was reconstructed, which is stratigraphically older than the Lithiotid Limestone Member from the exposed part of the modern quarry. During logging, samples of rock were taken from each bed. Thin sections (47 × 28 mm in size) were made from representative samples of each lithofacies. Finely ground surfaces of hand-specimens, as well as thin sections, were scanned with a high-resolution optical scanner. Thin sections were further investigated using a polarizing optical microscope. Limestone varieties were named according to classification by Dunham (1962), with modifications by Embry and Klovan (1971). In adding the components to the names of the samples we have followed the recommendations by Wright (1992) and express the predominant component first.

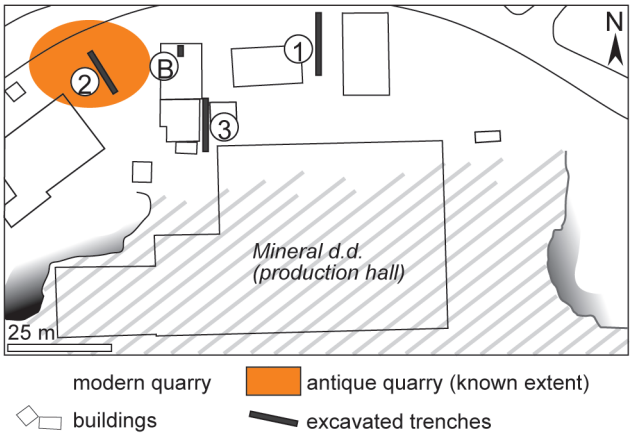

Fig. 3. Position of the excavated probes (archaeological trenches) that re-exposed the Roman quarry. The numbers 1–3 of the probes refer to sedimentary section logs presented in Fig. 5. Letter B denotes the outcrop in the basement of the house Podpeč 44.

The colour of the dry, broken surface of the stone was determined using the standardised Rock Color Chart (Munsell Color, 2010).

Mineralogical composition, concentrations of major, minor, and trace elements, and the isotopic composition of strontium, oxygen, and carbon isotopes of the samples from the ancient part of the quarry were measured. The analysis was performed on bulk rock samples. All secondary features (calcite veins, void fillings) were removed from the samples to obtain the geochemical values of the rock matrix.

Mineralogical composition was determined for seven samples. From each sample, 5 g of the rock was powdered and analysed with an X-ray diffractometer (XRD) Philips PW3710 under the following conditions: power 1.2 kW, voltage 40 kV, current 30 mA, wavelength of X-ray light with copper tube and Kα-rays 1.5460 Å. A secondary graphite monochromator and a proportional counter were used. The continuous recording range was 2° – 70° 2θ, at a rate of 3°/min. The mineralogical composition of the samples was determined using the X'Pert Highscore Plus computer programme. The measurements and analysis were carried out at the University of Ljubljana, Faculty of Natural Sciences and Engineering, Department of Geology.

Concentrations of major, minor, and trace elements were measured in Actlabs (Canada) from 16 samples (each weighing 5 g) using Fusion-ICP-MS. The accuracy of the measurements was ensured by certified lab standards, while precision was ensured by duplicating measurements. All values reported deviate from replicate samples by less than 2.15 %.

Samples for stable isotope values of $\delta^{18}O$ and $\delta^{13}C$ were taken in 90 cm intervals or less. Isotope values were measured for 37 samples (1 g in size) at the GeoZentrum Nordbayern laboratory at the University of Erlangen, Germany, using a Gasbench II connected to a ThermoFisher Delta V Plus mass spectrometer (Rosenbaum & Sheppard, 1986; Kim & Taylor, 2007). Results are given in the notation δ‰ (per mil) with respect to the international PDB scale. Reported reproducibility of the calibration standards was 0.05 SD for $\delta^{13}C$ and 0.04 SD for $\delta^{18}O$ isotope measurements. The effects of diagenesis were checked by cross-plotting the oxygen ($\delta^{18}O$) and carbon ($\delta^{13}C$) values.

Strontium ($^{87}Sr/^{86}Sr$) isotope values from seven samples were prepared and measured according to the laboratory procedure (Romaniello et al., 2015) at the Department of Earth Sciences, University of Oxford, and measured by a multi-collector inductively-coupled plasma mass spectrometer (MC-ICP-MS) using a standard bracketing method and the NIST SRM 987 standard (Weis, et al., 2006). Each sample was measured three times. The instrument mass fractionation was internally corrected to $^{86}Sr/^{88}Sr = 0.1194$. All reported $^{87}Sr/^{86}Sr$ ratios were normalised to SRM 987 $^{87}Sr/^{86}Sr = 0.710248$ (McArthur et al., 2012a). The external reproducibility of $^{87}Sr/^{86}Sr$ using the NIST SRM 987 standard (Weis, et al., 2006) yielded a value of 0.710251 ± 0.000025 (2SD, n=30). The measured ratios were correlated with the Locally Weighted Regression Scatterplot Smoother (LOWESS) fit curve constructed by McArthur et al. (2012b).

In addition, stone products kept by the National Museum of Slovenia (samples marked as NMS), and the Museum in Ljubljana (samples marked as MGML) were analysed following the multi-method approach (n=4) by using the same methods as described above. In addition, the minimum bed thickness required to produce the stone products studied was determined based on the unworked back-side of the product, which corresponds to the bedding plane.

Results

Geological map of Podpeč – St. Ana area

The mapped area is characterised by the presence of Mesozoic carbonates and various faults and folds (Fig. 4a). Upper Triassic Main Dolomite Formation outcrops only in the westernmost part of the mapped area, while the lowermost Jurassic Krka Limestone Member occurs in the northeasternmost part. Both are in fault contact with the rest of the Lower and Middle Jurassic succession. The Lithiotid Limestone Member was mapped as a single unit consisting of an abundance of medium grey biogenic limestones. Where possible, this unit was further subdivided into the Orbitopsella Limestone Member (recognised by dark grey micritic, peloidal, and biogenic limestones without lithiotid bivalves), the Lithiotid Limestone Member, and the Oolithic Limestone Member. To the south, the Lithiotid Limestone Member or Oolithic Limestone Member passes into the Spotty Limestone Member. The Spotty Limestone Member is characterised by dark grey, thin-bedded, nodular oolithic and/or crinoidal limestones with rare micritic parts. It gradually passes into the Middle Jurassic Laze Formation. This unit consists of medium- to thick-bedded, sometimes even massive oolithic carbonates. Limestone varieties predominate at Podpeč, while mainly dolomitized oolithic limestone outcrops on the slopes of the St. Ana Hill and in the westernmost parts. The succession is dissected by strike slip and normal faults, and a SW plunging syncline was inferred from changes in the strike and dip direction of the beds. The shape of the surface is strongly modified by human activities (Fig. 4b). Numerous abandoned quarries can be found along the entire northeastern, northern, and northwestern slopes of the St. Ana hill, extending up to 100 m above the Barje basin.

Description of sedimentological sections

The archaeological trenches exposed almost 32 m of the limestone succession. Since some trenches were positioned lateral to each other, the stratigraphic thickness of the exposed outcrops totals 23 m. Bedding planes dip at 70°–80° towards the south. Some minor fissures are present, but we could not detect any off-sets of the beds.

Two facies assemblages can be defined – the first for the lower part of the succession (probes 1 and 2, and short section Basement Podpeč 44), and a second for the upper part of the logged succession (probe 3).

Facies assemblage 1 can be defined on the prevailing occurrence of dark varieties of micritic limestone (Fig. 5). A lower energy environment can be defined for this part, interrupted occasionally by high energy events. Although probes 1 and 2 are nearly parallel to each other and perpendicular to the bedding, the logged sections differ in the thickness of the beds and to some

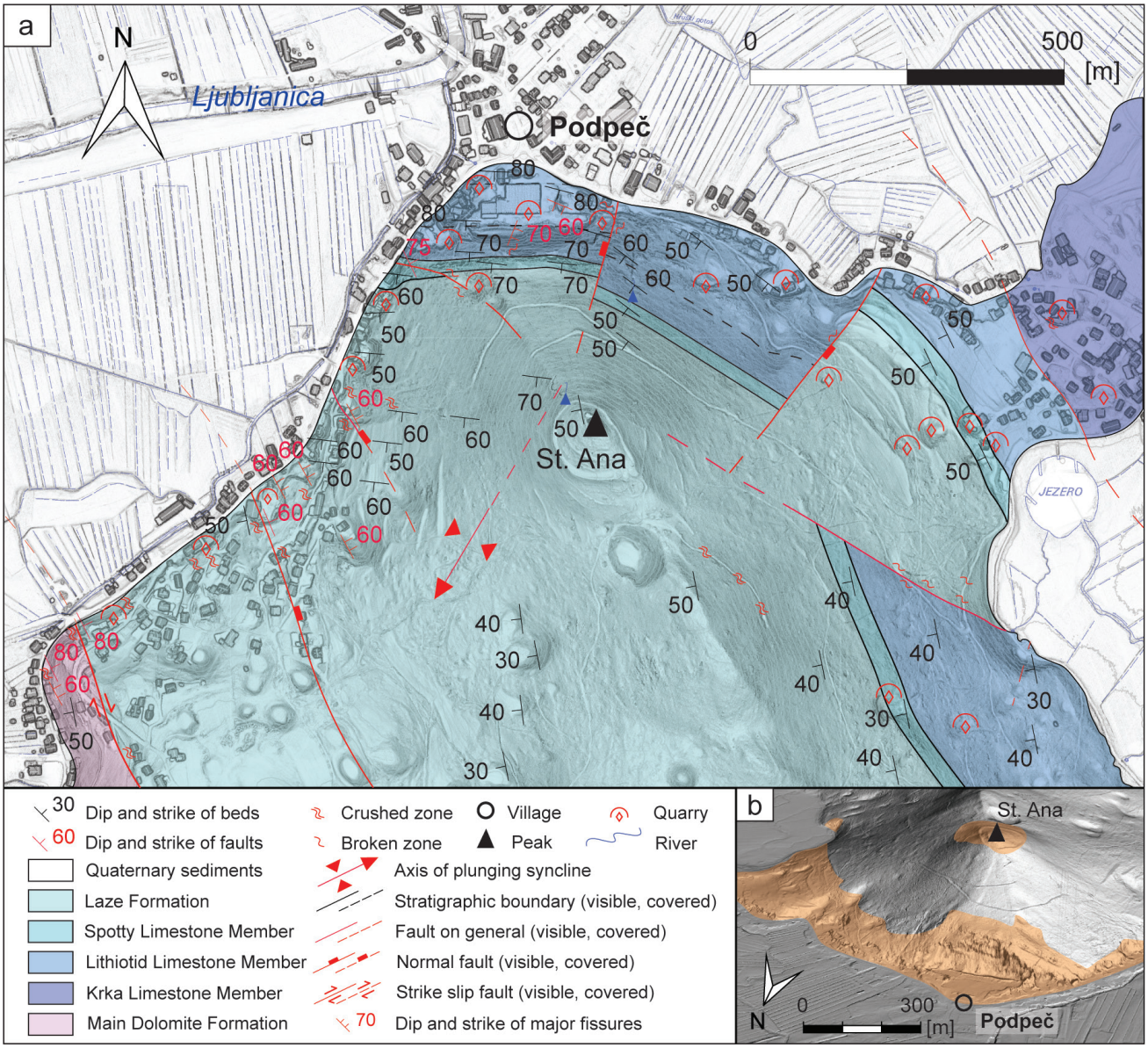

Fig. 4. a – Geological map on the scale 1: 5000 of Podpeč – St. Ana area; b – digital elevation model of Podpeč – St. Ana with marked anthropogenically altered areas. The source of the topography is a 1 m × 1 m resolution digital relief model (The Surveying and Mapping Authority of the Republic of Slovenia, 2011).

extent also in their microfacies, so the correlation between the beds is not entirely straightforward. The reason for the differences among the sections is most likely due to lateral changes in microfacies (e.g. the microfacies with megalodontid bivalves likely represents storm deposits, which may laterally pinch out), the limited availability of the outcrop (trenches were only a few decimetres wide, so some fissures could be mistaken for bedding planes, and vice-versa), or (less likely) due to some minor fault. Despite this, the microfacies association in probes 1 and 2, as well as from the section logged in the basement of House Podpeč 44, is the same: dark micritic and fine-grained facies (microfacies 4 and 5) and limestone with bivalves predominates (microfacies 13 and 14) over microfacies with oncoids or ooids (microfacies 9–11).

Fig. 5. Sedimentological section in the scale 1: 50 of the antique quarry. Abbreviations for the textures: M- mudstone, W- wackestone, P- packstone, G- grainstone, F- floatstone, R- rudstone. Note that the facies are numbered somewhat differently than in Djurić et al. (2022) and that more varieties are distinguished here.

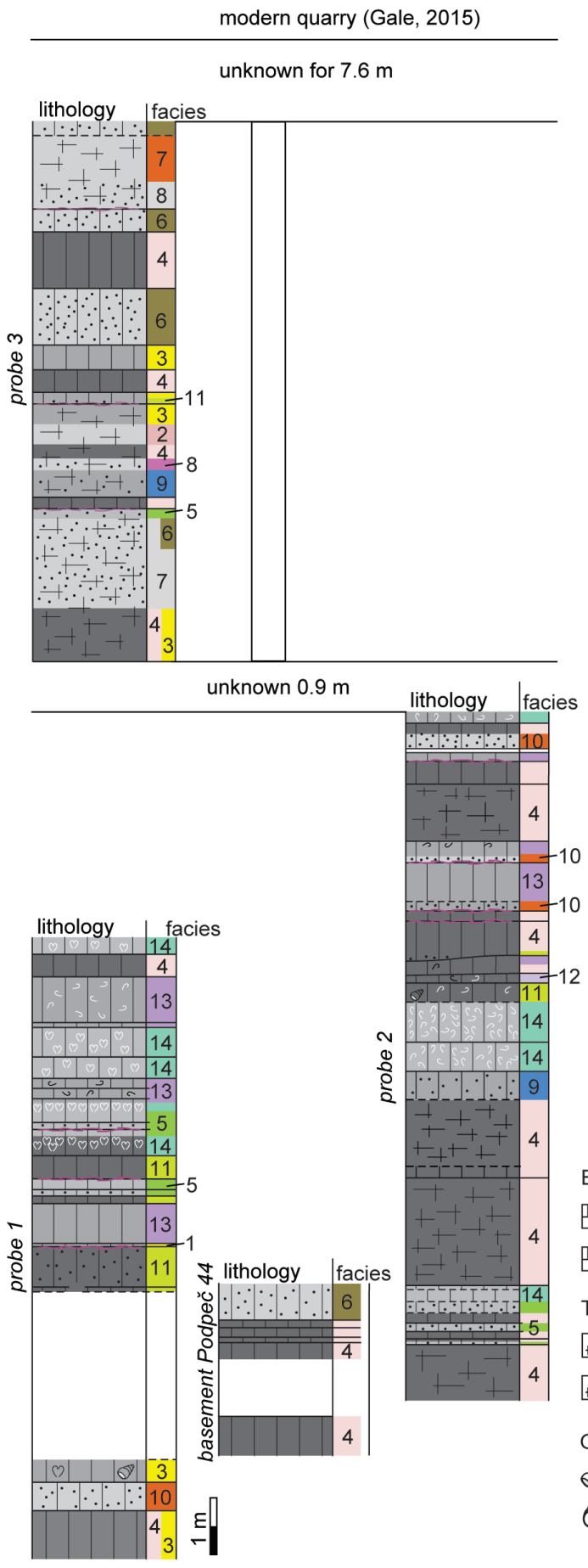

Facies types:

MICRITIC LIMESTONE

1 light brownish grey M

2 med. grey fenestral M

3 med. dark grey bioclastic W

4 dark grey pelletal-bioclastic W

FINE-GRAINED LIMESTONE

5 med. dark grey peloid G with rare large bivalves

6 med. grey to olive grey intraclastic-bioclastic W/P

OOLITHIC LIMESTONE

7 med. grey to olive grey ooid G with rare cortoids

8 med. grey ooid G; large ooids

9 med. dark grey ooid G; small ooids

ONCOID/CORTOID LIMESTONE

10 med. dark grey cortoid F with intraclastic-bioclastic W/P matrix

11 dark grey oncoid F with peloid W/P matrix

12 dark grey oncoid F; *Thaumatoporella* W matrix

LIMESTONE WITH BIVALVES

13 med. dark grey bivalve F with small shells and peloid G matrix

14 (med.) dark grey megalodontid F/R with micritic matrix

Lithology:

BEDDED LIMESTONE (bed-thickness < 1 m)

micritic/fine-grained limestone

calcarenite

THICK-BEDDED LIMESTONE (bed-thickness > 1 m)

micritic/fine-grained limestone

calcarenite

GRAINS

gastropods bivalves

brachiopods clayey surface

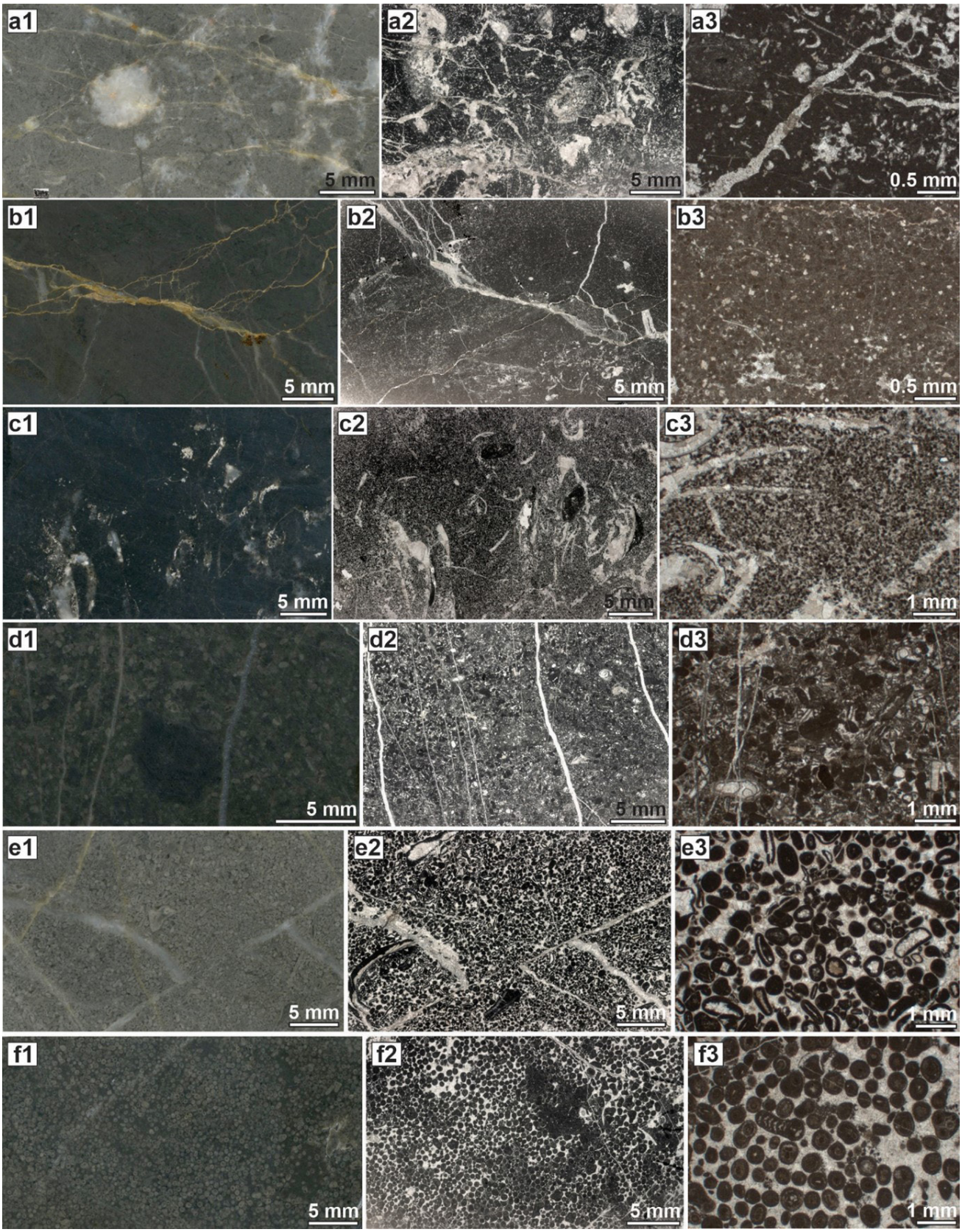

Fig. 6. Microfacies (MF) of limestone from the antique quarry at Podpeč. Numbers indicate polished surface of the stone in reflected light (1), thin section scan (2), and microphotograph of the same sample (3). a: Medium grey bioclastic wackestone (MF 3). Thin section 1689. b: Dark grey pelletal- bioclastic wackestone (MF 4). Thin section 1677. c: Medium dark grey peloid grainstone with rare larger bivalves (MF 5). Thin section 1683. d: Medium grey to olive grey intraclastic-bioclastic wackestone and packstone (MF 6). Thin section 1684. e: Medium dark grey ooid grainstone; with rare cortoids (MF 7). Thin section 1686. f: Medium dark grey ooid grainstone; large ooids (MF 8). Thin section 1691.

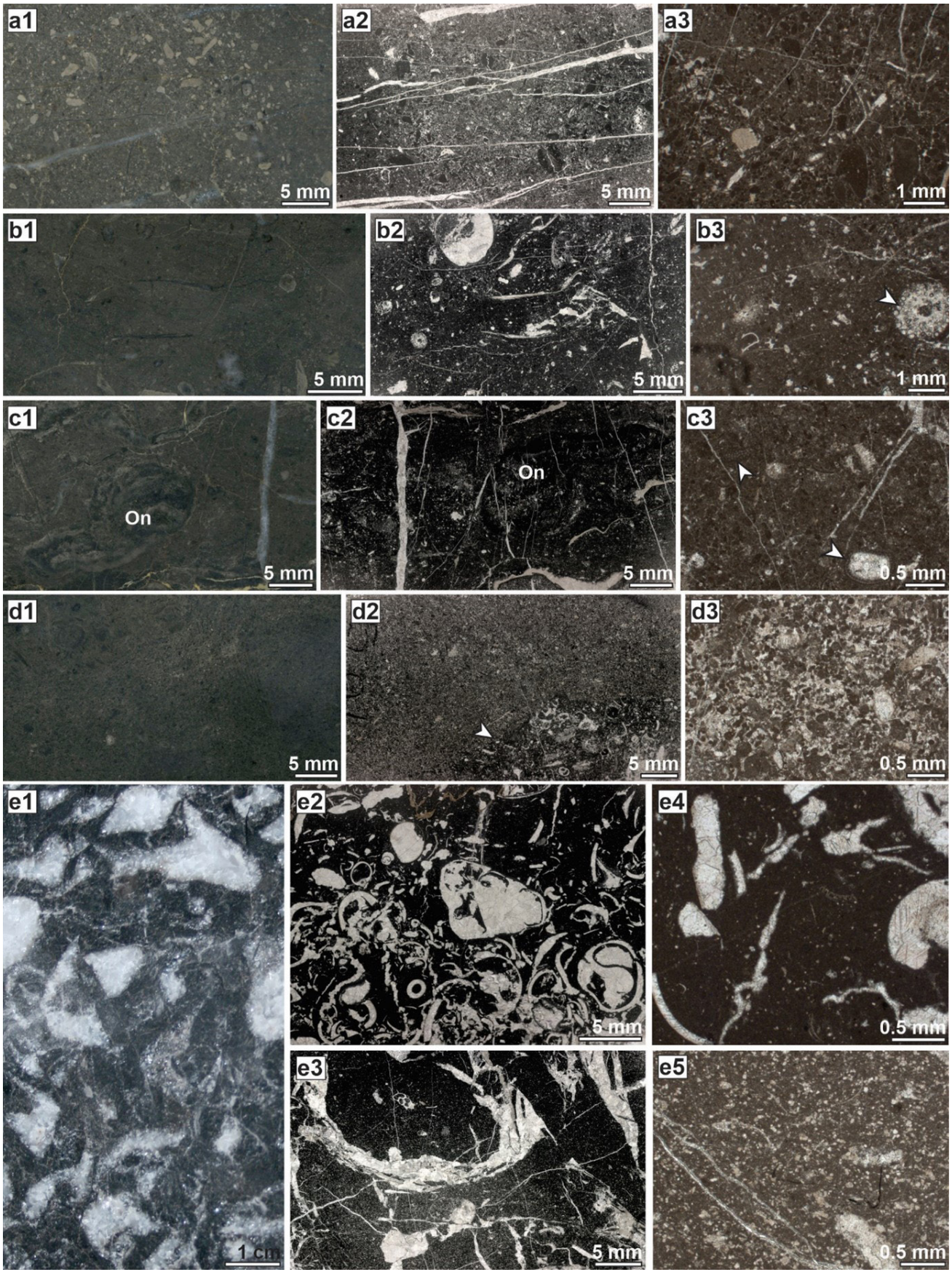

Fig. 7. Microfacies of limestone from the antique quarry at Podpeč (*continued*). a: Medium dark grey cortoid floatstone with intraclastic-bioclastic wackestone and packstone matrix (MF 10). Thin section 1690. b: Dark grey oncoid floatstone with peloid wackestone to packstone matrix (MF 11). Arrow in *b3* is pointing at the dasycladacean algae. Thin section 1681. c: Dark grey oncoid floatstone with *Thaumatoporella* wackestone matrix (MF 12). *On* indicates an oncoid. Arrows point at *Thaumatoporella*. Thin section 1688. d: Medium dark grey bivalve floatstone with small shells and peloid grainstone matrix (MF 13). Arrow points at an irregular contact with bivalve floatstone. Thin section 1680. e: (Medium) dark grey megalodontid floatstone to rudstone with micritic matrix (MF 14). Photos *e2* and *e4* are from a variety with mudstone matrix (thin section 1687), while *e3* and *e5* contain small particles of shells within the matrix (thin section 1682).

The upper part of the logged succession is attributed to facies assemblage 2. Lighter varieties of oolithic limestone (microfacies 7–9) become common along with micritic limestone. No shell deposits were found in the stratigraphically highest probe 3. A higher energy environment of sedimentation was interpreted for facies assemblage 2, based on the larger presence of oolithic limestones. Due to the higher energy setting, foraminifera assemblages within the oolithic microfacies cannot be considered autochthonous but are rather parautochthonous.

The microfacies are documented in Figures 6–7 and described in detail in Table 1.

Table 1. Description of microfacies from the antique quarry at Podpeč. The most abundant and diagnostic fossil taxa are underlined.

Microfacies	Description	Bed thickness (min–max; in cm	Figure
1 light brownish grey mudstone	Micritic limestone with almost complete predominance of micritic matrix and less than 10 % of clasts.	4 - 18	/
2 medium grey fenestral mudstone	Mudstone with irregular fenestrae.	40 - 100	/
3 medium grey bioclastic wackestone	The amount of small bivalve shells within this heterogenous bioclastic wackestone varies from 10 to 50 %. Most are 0.3 mm in length. The original mineral was dissolved and replaced by calcite spar. Gastropods, echinoderms, ostracods, and foraminifera are subordinately present. The intergranular space is filled with dense micritic matrix. Small corrosion vugs and putative small neptunian dykes/desiccation cracks, filled with crystal silt, intraclasts and fragments of spar are also present. The foraminiferal assemblage comprises *Siphovalvulina* sp. and Textulariidae.	40 - 85	5a
4 dark grey pelletal-bioclastic wackestone	Sample is heterogeneous. Two microfacies types can be distinguished, but with intermediate transitions. Most of the rock is represented by bioclastic-pelletal wackestone with a few (0.5 %) clasts of larger size (gastropod and bivalve shells). Wackestone consists of 15 % of grains: small angular sparitic fragments, ostracods, and small (0.08 mm) rounded pellets. Ostracod valves are separated or still closed. The other end member is also a pelletal-bioclastic wackestone, but with pellets representing 30-40 % of the rock, and bioclasts (echinoderms, bivalve fragments, small *Siphovalvulina* foraminifera) amounting to 5-10 %. Wackestones contain some irregular vugs and cracks filled with pellets, microspar and cement. Some of these might be desiccation cracks and vugs, while some might be caused by bioturbation. Larger gastropod and bivalve shells are filled with crystal silt and drusy mosaic cement.	10 - 120	5b
5 medium dark grey peloid grainstone with rare larger bivalves	Large (1 cm or longer) bivalve shells and very rare intraclasts within the peloid cortoid grainstone matrix represent less than 10 % of the rock. Shells are altered to drusy mosaic spar and exhibit micritic outer rim (cortoids). The grainstone consists of peloids, which measure 0.08 – 0.12 mm in size and are very well sorted. They represent 90–95 % of the grains, disregarding the mentioned larger bivalve shells. Ostracods, foraminifera (?Valvulinidae), *Thaumatoporella,* echinoderm fragments, and undeterminable sparitic particles are subordinate.	10 - 25	5c
6 medium grey to olive grey intraclastic-bioclastic wackestone and packstone	Heterogeneous texture is wackestone to packstone in nature. Grains are very poorly sorted and matrix-supported or in point contacts. Intraclasts (20–40 % of grains) are micritic, rounded, circular to semi-elongated. Some micritised ooids are also present, but difficult to distinguish from intraclasts. Approximately 10 % of the volume is occupied by bivalve shells. These are fragmented, abraded and have micritised margins (cortoids). *Thaumatoporella* is present in up to 5 % of the volume. Foraminifera represent 1–2.5 % of the rock. Gastropods, echinoderms, brachiopods, ostracods, and fragments of dasycladacean algae are sporadically present. Micritic matrix is locally partly washed away, and the intergranular space is locally filled with drusy mosaic cement. Foraminifera are represented by Valvulinidae, *Meandrovoluta asiagoensis* Fugagnoli & Rettori, *Siphovalvulina* spp., *Duotaxis metula* Kristan, and *Gaudryina* sp.	25 - 100	5d
7 medium dark grey ooid grainstone with rare cortoids	Moderately well sorted mature ooids and superficial ooids form almost 50 % of the rock volume and are the predominating grain type. They are in point contacts with each other and grains of other types. The mature ooids are concentric, with tangential structure. Their cores are mostly micritised. Foraminifera and sparitic particles rarely served as basis for the ooids' formation. Their average size is 0.5 mm. Less numerous are superficial ooids with 6–7 laminae, mostly formed around elongated mollusc shell fragments up to 0.7 mm in length. Both types of ooids form lumps and mature lumps up to 1 mm in size. Fragments of echinoderms, benthic foraminifera and micritised bivalves (cortoids) are subordinate. The intergranular space is filled with drusy mosaic calcite cement. The foraminiferal assemblage consists of *Siphovalvulina* spp., Valvulinidae, Taxtulariidae, *Reophax* sp., ?*Haurania deserta* Henson, unidentified large benthic foraminifera with coarsely agglutinated wall, *Involutina farinacciae* Brönnimann & Koehn-Zaninetti.	13 - 85	5e

8 medium dark grey ooid grainstone; large ooids	Well sorted, 1 mm large ooids occupy approximately 50 % of the rock volume. Ooids were originally concentric but got slightly compacted during diagenesis and are now more ellipsoid in shape. Although their tangential structure is clearly recognisable, their inner regions show some recrystallization. Some were formed around sparitic fragments or foraminifera but have micritic cores. The laminar part is thick, representing approximately 45 % of the ooids' radius. Nine to twelve laminae are visible on the outer part of the cortices. Spiny ooids are very few. Some of the ooids are glued together into aggregate grains (lump and mature lump stage) up to 2.5 mm in diameter. Peloids are irregularly distributed among ooids and represent a little less than 10 % of the rock. They measure approximately 0.15 mm in size. Neomorphically altered bivalve fragments, foraminifera, gastropods, and echinoderm plates are very rare. The intergranular space is filled with drusy mosaic calcite cement. The foraminiferal assemblage consists of Lituosepta sp., ?*Haurania deserta* Henson, *Meandrovoluta asiagoensis* Fugagnoli & Rettori, *Lituolipora* sp., Textulariidae and Valvulinidae, *Pseudopfenderina butterlini* (Brun), small *Ophthalmidium* sp., and *Involutina farinacciae* Brönnimann & Koehn-Zaninetti.	32 - 40	5f
9 medium dark grey ooid grainstone; small ooids	The composition and texture are as in microfacies 8. The difference is in the size of the ooids: average diameter of ooids in this microfacies is 0.55 mm, and peloids measure 0.07 mm. Foraminiferal assemblage is identical.	28 - 50	/
10 medium dark grey cortoid floatstone with intraclastic-bioclastic wackestone and packstone matrix	The matrix is virtually indistinguishable from microfacies 6. The difference between the microfacies is in the greater abundance of larger clasts seen at the macroscopic level. Foraminifera are represented by Valvulinidae, *Meandrovoluta asiagoensis* Fugagnoli & Rettori, *Siphovalvulina* spp., *Haurania deserta* Henson, *Duotaxis metula* Kristan, *Pseudopfenderina butterlini* (Brun), Textulariidae, Valvulinidae, ?*Mesoendothyra* or ?*Everticyclammina* sp., and ?*Planiinvoluta* sp.	16 - 55	6a
11 dark grey oncoid floatstone with peloid wackestone to packstone matrix	Grains represent approximately 40 % of the rock volume. The rock is microscopically heterogenous, probably bioturbated (one cm-size burrow is clearly distinguishable, at the bottom filled with pelletal packstone and in the upper part by blocky spar). Peloids are of variable sizes, ranging from 0. 08–0.12 mm to 1 mm. The largest may be recognised as intraclasts. Most peloids are spherical to half-spherical, rounded to well rounded. They represent 20–30 % of the volume. Some of the sphaerical peloids are likely micritised ooids. Their size ranges from 0.2 to 0.4 mm. Other grains are subordinate: foraminifera and thalli of *Thaumatoporella* each form 1–2.5 % of the rock. Up to 2 mm long fragments of dasycladacean algae are irregularly distributed, on the edges micritised and partly overgrown by microbialites. Only one, at the edges heavily micritised and partly overgrown by *Thaumatoporella*, bivalve shell was recognised. Ostracods, echinoderm plates and gastropods are also very rare (1 %). Part of the micritic matrix has been washed away, but some of the vugs could also represent desiccation pores. Vugs are filled with drusy mosaic calcite cement. The foraminiferal assemblage consists of *Meandrovoluta asiagoensis* Fugagnoli & Rettori, *Siphovalvulina* spp., Valvulinidae, and *Earlandia* sp. Remarks: Compared to the matrix in microfacies 12, and microfacies 13, these microfacies contains less *Thaumatoporella* grains and the greater presence of *Meandrovoluta*.	13 - 33	6b
12 dark grey oncoid floatstone with *Thaumatoporella* wackestone matrix	Oncoids are 2 cm in size, constructed of homogenous micrite, *Thaumatoporella* and calcimicrobes. Locally present are bivalve shells, which are heavily bioeroded and overgrown by microbialite. Large grains float in partly washed peloid-bioclastic wackestone (grains represent 10-30 % of surface) matrix with common thalli of *Thaumatoporella*. The latter may represent up to 10 % of the volume. Other bioclasts are large benthic foraminifera (5 %) and rare gastropods. Peloids and intraclasts are also abundant. Peloids range from 0.05 to 0.1 mm in size and are rounded, while intraclasts are sub-rounded and have an average size of 0.2 mm. Micritic matrix is in some places clotted. The foraminiferal assemblage consists of Valvulinidae, *Siphovalvulina* spp., *Meandrovoluta asiagoensis* Fugagnoli & Rettori, and *Duotaxis metula* Kristan.	13 - 70	6c
13 medium dark grey bivalve floatstone with small shells and peloid grainstone matrix	The matrix is identical to facies 5. The distinction is at the macroscopic level, as the microfacies 13 contains bivalve shells representing more than 10 % of the rock volume. Within the thin section made and shown in Figure 6d, the grainstone is in irregular contact with bivalve floatstone (shells 2.5 mm in size) with bioclastic wackestone matrix. Besides bivalve shells and fragments of dasycladacean algae, gastropods, echinoderms, foraminifera (*Siphovalvulina* and a dubious *Ammobaculites*), and calcimicrobes are less commonly present.	16 - 80	6d
14 (medium) dark grey megalodontid floatstone to rudstone with micritic matrix	Large (0.5–3 cm large) shells of bivalves and gastropods form 15–50 % of the rock volume. They are replaced by clear drusy mosaic spar. Micritic matrix contains rare ostracods, fragments of dasycladacean algae, some *Thaumatoporella* thalli, and calcimicrobes. Foraminifera are small and very rare. Very small fragments of bivalve shells may be locally more common, filling between 20 and 30 % of space.	24 - 72	6e

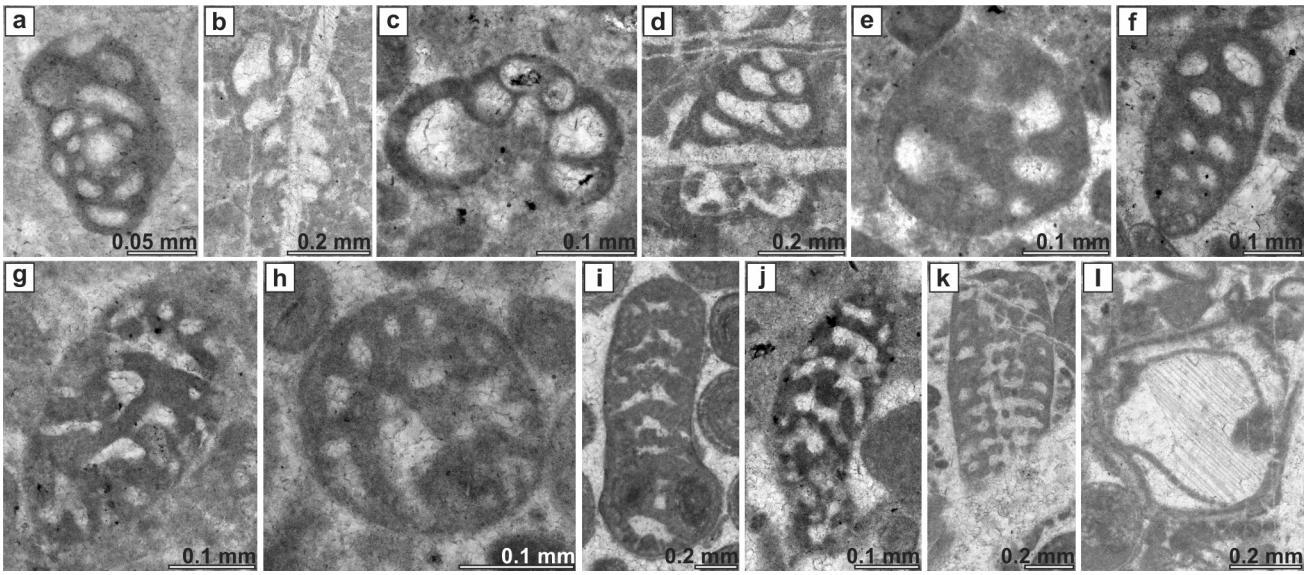

Fig. 8. Foraminifera from the Pliensbachian limestone in the antique quarry at Podpeč. a: *Meandrovoluta asiagoensis* Fugagnoli & Rettori. Thin section 1679. b: *Siphovalvulina* cf. *variabilis* Septfontaine. Thin section 1684. c: *Siphovalvulina gibraltarensis* BouDagher-Fadel, Rose, Bosence & Lord. Thin section 1679. d: *Duotaxis metula* Kristan. Thin section 1684. e: *Pseudopfenderina butterlini* (Brun). Transverse section. Thin section 1679. f: *Pseudopfenderina butterlini* (Brun). Oblique longitudinal section. Thin section 1679. g: *Amijiella amiji* (Henson). Oblique longitudinal section. Thin section 1679. h: *Amijiella amiji* (Henson). Oblique transverse section. Thin section 1679. i: *Lituolipora* sp. Longitudinal section. Thin section 1678. j: *Lituosepta* sp. Longitudinal section. Thin section 1679. k: ?*Lituosepta* sp. Longitudial section. Thin section 1678. l: *Thaumatoporella* sp. Thin section 1684.

Foraminiferal assemblages

The most abundant foraminiferal taxa in each microfacies are underlined in Table 1 and presented in Figure 8. Only *Siphovalvulina* and small Textulariidae are present in bioclastic wackestone and in pelletal-bioclastic wackestone. Peloid grainstone with rare bivalve shells, where only Valvulinidae are present, alongside with problematic algae *Thaumatoporella*. Intraclastic-bioclastic wackestone and packstone is characterised by the abundance of Valvulinidae and *Meandrovoluta asiagoensis*. Cortoid floatstone with intraclastic-bioclastic wackestone and packstone matrix contains an abundance of Valvulinidae, *Meandrovoluta asiagoensis*, *Siphovalvulina* spp., and *Haurania deserta*. Oncoid floatstone with peloid wackestone to packstone matrix commonly contains *Meandrovoluta asiagoensis* and *Siphovalvulina* spp., but, unlike the dark grey oncoid floatstone with *Thaumatoporella* wackestone matrix, it has much less of the *Thaumatoporella*. Foraminifera in bivalve and megalodontid floatstone are too few to be considered diagnostic for these facies. Based on the presence of *Lituosepta* and the absence of *Orbitopsella*, we tentatively place the logged succession in the late Sinemurian *Lituosepta recoarensis* lineage zone (Kabal & Tasli, 2003; Velić, 2007). However, *Orbitopsella* might also be absent due to environmental factors.

Mineralogical, geochemical, and isotopic characterisation of the ancient Podpeč quarry

XRD analysis of the limestone revealed only the presence of calcite (Fig. 9a) due to mineralogical purity of the studied samples and method detection limits. Table 2 lists concentrations of major oxides, minor elements, trace elements above detection limits, and isotope values of $\delta^{13}C$, $\delta^{18}O$, $^{87}Sr/^{86}Sr$. The limestone is characterised by a high CaO content and a low MgO content, as is expected for pure limestones. SiO_2 is positively correlated with Al_2O_3, K_2O and TiO (linear correlation coefficients r = 0.87, r = 0.76, and r = 0.54 respectively; number of samples n = 15). By cross-plotting the $\delta^{18}O$ and $\delta^{13}C$ isotope ratios it was found that only two samples indicate the influence of early meteoric diagenesis (Fig. 9b). These samples were eliminated from any further analysis. Strontium isotope data from the Lithiotid Limestone Member measured at the ancient Podpeč quarry were plotted on a box and whiskers diagram and correlated with a global strontium curve (Fig. 9c).

The local isotope curves of $\delta^{18}O$ and $\delta^{13}C$ are shown on a composite log in Figure 10. The carbon isotope compositions range from -2.44 ‰ to 2.5 ‰ (n=37) for micritic limestone, 0.28 ‰ to 1.84 ‰ (n=6) for fine-grained limestone, -0.21 ‰ to 0.93 ‰ (n=6) for oolithic limestone, -0.07 ‰ to 1.12 ‰ (n=2) for oncoid/cortoid limestone, and 0.02 ‰ to 1.95 ‰ (n=8) for limestone with bi-

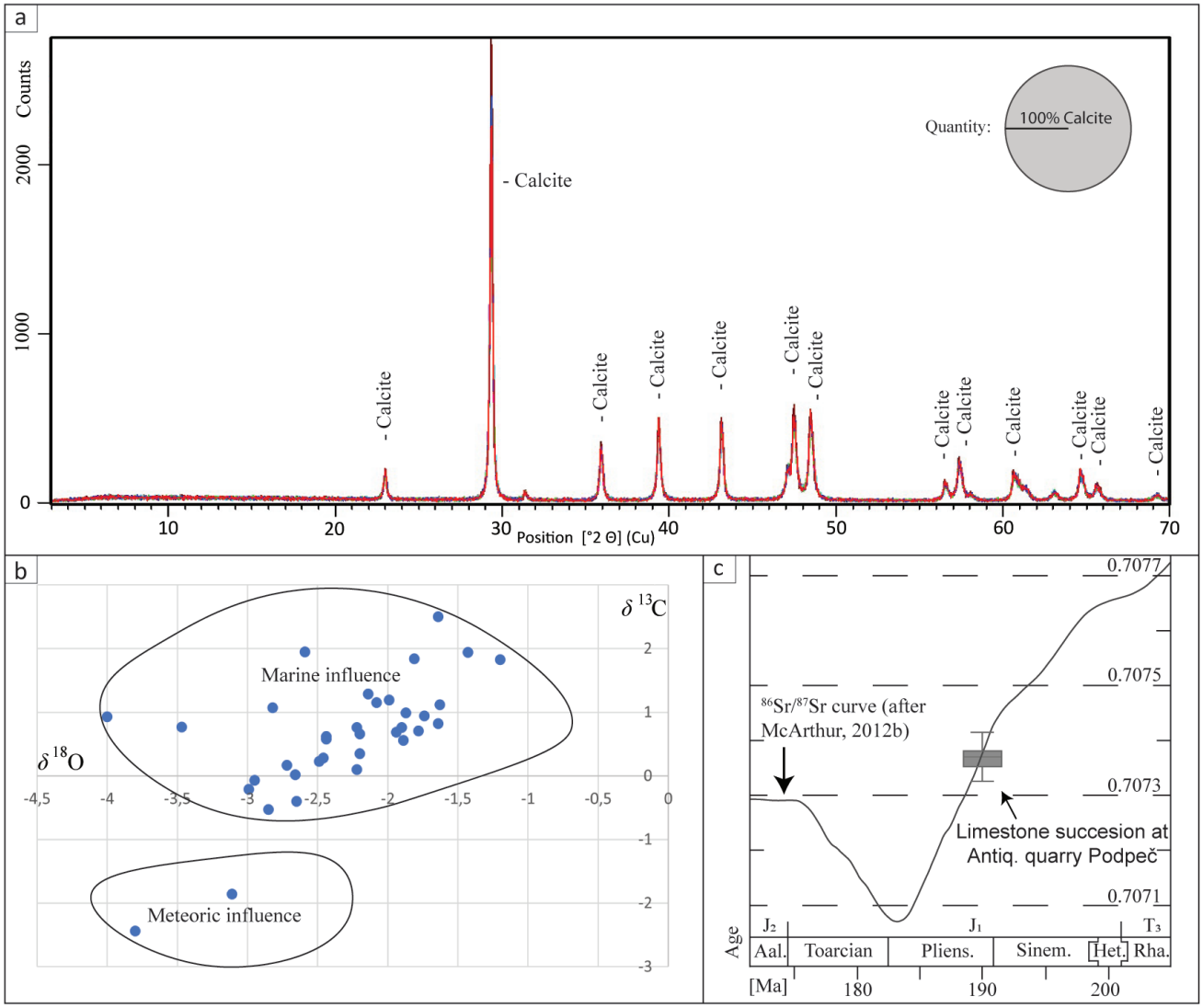

Fig. 9. Mineralogical, geochemical and isotope characterisation of antique part of Podpeč quarry. a: XDR mineralogical composition of the studied samples. Only calcite shows on all of the roentgenograms (n=7). b: $\delta^{13}C$ and $\delta^{18}O$ cross scatter plot of diagenesis in the studied samples. Blue circles represent the individual measurements plots. c: Box and whiskers graph of $^{87}Sr/^{86}Sr$ values of samples from antique part of Podpeč quarry correlated with the global Sr curve from McArthur et al. (2012b).

valves. Unique values can be reported only for micritic limestones in the range from -2.44 ‰ to -0.21 ‰ and 1,95 ‰ to 2,5 ‰. The oxygen isotope compositions range from -3.8 ‰ to -1.2 ‰ (n=37) for micritic limestone, from -2.82 ‰ to -1.81 ‰ (n=6) for fine-grained limestone, from -4 ‰ to -1.78 ‰ (n=6) for oolithic limestone, from -2.95 ‰ to -1.63 ‰ (n=2) for oncoid/cortoid limestone, and from -2.72 ‰ to -1.87 ‰ (n=8) for limestone with bivalves. Values recorded in only one facies in oolithic limestone range from -4 ‰ to -3,8 ‰ and for micritic limestone facies from -1.63 ‰ to -1.2 ‰.

The $^{87}Sr/^{86}Sr$ isotope values within the succession in the antique quarry decrease from 0.707414 to 0.707329 (Table 2).

Geological characterisation of stone products and its provenance determinations

The stone products MGML 48572, MGML 51180, NMS L209 and NMS 210 belong to microfacies 2 (micritic limestone), 6 (fine-grained limestone), 7 and 9 (oolithic limestone) respectively (for facies descriptions see Table 1). Multi-method data acquired from the analysis of the stone products are listed in Table 3. As in primary samples also the studied stone products are characterised by the high CaO and low MgO content. Linear correlation (n = 4) was analysed only between SiO_2 with Al_2O_3, K_2O and TiO_2 to check the previously determined correlation from primary samples also in stone products. Linear correlation coefficients between SiO_2 with Al_2O_3

Table 2. Geochemical values of major (oxides), minor, and trace elements with measured concentration above detection limit and $\delta^{13}C$, $\delta^{18}O$, $^{87}Sr/^{86}Sr$ isotope values for the Lower Jurassic limestone in the antique quarry at Podpeč.

Position of the sample in the succession (m from the base)	Microfacies (see Fig. 4)	SiO_2 [wt%]	Al_2O_3 [wt%]	Fe_2O_3 [wt%]	MnO [wt%]	MgO [wt%]	CaO [wt%]	Na_2O [wt%]	K_2O [wt%]	TiO_2 [wt%]	LOI [wt%]	Sr [ppm]	Zr [ppm]	U [ppm]	$\delta^{13}C$	$\delta^{18}O$	$^{87}Sr/^{86}Sr$ (2SD)
0.5	3	0.31	0.14	0.05	0.004	0.69	55.79	0.05	0.03	0.002	43.43	280	3	2.1	2.50	-1.64	0.707414 (0.000003)
1.1	10	/	/	/	/	/	/	/	/	/	/	/	/	/	0.76	-2.22	/
1.6	2	0.33	0.16	0.05	0.005	0.44	56.32	0.06	0.03	0.002	43.36	120	2	2.6	-0.53	-2.85	/
2.7	4	0.37	0.18	0.07	0.006	0.57	55.99	0.05	0.05	0.005	43.23	149	3	3.5	0.10	-2.22	/
3.3	14	/	/	/	/	/	/	/	/	/	/	/	/	/	0.69	-1.94	/
3,8	4	/	/	/	/	/	/	/	/	/	/	/	/	/	0.94	-1.74	/
4.0	3	0.37	0.18	0.09	0.005	0.73	54.73	0.05	0.04	0.005	43.41	270	3	2.9	1.94	-1.43	0.707377 (0.000006)
4.5	3	0.34	0.16	0.08	0.004	0.67	55.25	0.06	0.04	0.003	43.5	248	3	4.9	1.83	-1.20	/
5.4	1	/	/	/	/	/	/	/	/	/	/	/	/	/	-1.86	-3.11	/
5.6	4	0.44	0.23	0.05	0.007	0.67	53.33	0.06	0.03	0.002	43.53	178	7	3.7	0.82	-1.64	/
5.9	12	/	/	/	/	/	/	/	/	/	/	/	/	/	-0.07	-2.95	/
6.3	4	/	/	/	/	/	/	/	/	/	/	/	/	/	0.35	-2.20	/
6.4	5	/	/	/	/	/	/	/	/	/	/	/	/	/	1.84	-1.81	/
6.6	14	/	/	/	/	/	/	/	/	/	/	/	/	/	1.19	-1.99	/
6.9	11	0.43	0.2	0.12	0.005	0.54	54.42	0.06	0.04	0.003	43.44	140	3	2.8	/	/	/
7.3	14	0.39	0.19	0.08	0.005	0.6	55.63	0.05	0.04	0.004	42.56	193	3	2.7	1.95	-2.59	/
7.8	8	/	/	/	/	/	/	/	/	/	/	/	/	/	0.58	-2.44	/
8.0	14	/	/	/	/	/	/	/	/	/	/	/	/	/	0.99	-1.87	/
8.3	12	/	/	/	/	/	/	/	/	/	/	/	/	/	1.12	-1.63	/
8.7	13	/	/	/	/	/	/	/	/	/	/	/	/	/	0.02	-2.66	/
9.1	14	/	/	/	/	/	/	/	/	/	/	/	/	/	1.29	-2.14	/
9.4	13	/	/	/	/	/	/	/	/	/	/	/	/	/	0.23	-2.49	/
9.7	13	/	/	/	/	/	/	/	/	/	/	/	/	/	0.17	-2.72	/
10.4	3	0.55	0.37	0.07	0.005	0.57	54.22	0.08	0.09	0.005	43.38	174	4	2.8	0.76	-1.90	0.707375 (0.00004)
10.9	4	0.38	0.19	0.1	0.005	0.6	55.25	0.05	0.05	0.005	43.24	177	3	4.3	0.62	-2.44	/
12.3	6	/	/	/	/	/	/	/	/	/	/	/	/	/	0.66	-2.20	/
14.9	10	0.41	0.19	0.07	0.005	0.64	54.7	0.06	0.04	0.003	43.54	207	3	3	0.93	-4.00	/
15.8	5	/	/	/	/	/	/	/	/	/	/	/	/	/	1.07	-2.82	/
16.7	9	/	/	/	/	/	/	/	/	/	/	/	/	/	0.77	-3.47	/
17.6	2	/	/	/	/	/	/	/	/	/	/	/	/	/	-2.44	-3.80	/
18.2	3	/	/	/	/	/	/	/	/	/	/	/	/	/	-0.40	-2.65	/
18.9	6	0.39	0.19	0.06	0.005	0.53	55.31	0.05	0.05	0.004	43.42	138	3	3	0.28	-2.46	0.707332 (0.000011)
19.4	6	/	/	/	/	/	/	/	/	/	/	/	/	/	0.56	-1.89	/
20.6	8	0.55	0.24	0.06	0.005	0.5	54.47	0.09	0.05	0.003	43.45	165	3	2.8	-0.21	-2.99	/
21.7	7	0.44	0.21	0.06	0.006	0.63	54.6	0.06	0.05	0.004	43.23	172	3	1.4	0.71	-1.78	0.707329 (0.000012)
22.9	6	0.59	0.28	0.08	0.005	0.68	55.35	0.07	0.08	0.008	43.33	208	3	5.2	1.15	-2.08	/

Table 3. Geochemical values of major (oxides), minor, and trace elements with measured concentration above detection limit and $\delta^{13}C$, $\delta^{18}O$, $^{87}Sr/^{86}Sr$ isotope values for the studied stone products (see Djurić et al, 2022 for complete set of the studied stone products).

Inventory number (use)	Micro-facies (see Fig. 5)	Minimal bed thick-ness [cm]	SiO_2 [wt%]	Al_2O_3 [wt%]	Fe_2O_3 [wt%]	MnO [wt%]	MgO [wt%]	CaO [wt%]	Na_2O [wt%]	K_2O [wt%]	TiO_2 [wt%]	LOI [wt%]	Sr [ppm]	Zr [ppm]	U [ppm]	$\delta^{13}C$	$\delta^{18}O$	$^{87}Sr/^{86}Sr$ (2SD)
MGML 48572 (Inscripti-on stone)	3	10 cm	1,19	0,61	0,23	0,005	0,61	54,47	0,04	0,17	0,029	42,53	134	7	2,4	0,44	-2,94	0,707352 (0,000077)
MGML 51180 (Inscripti-on stone)	6	43 cm	0,34	0,15	0,07	0,004	0,63	54,46	0,05	0,03	0,005	43,34	178	2	2,7	1,33	-1,12	0,707351 (0,000026)
NMS L209 (lorica)	7	30 cm	0,27	0,13	0,11	0,005	0,54	54,81	0,03	0,02	0,003	43,36	151	3	0,4	2,29	-3,17	0,707331 (0,000047)
NMS L210 (lorica)	9	30 cm	1	0,47	0,24	0,008	0,57	54,91	0,05	0,11	0,021	42,7	140	5	0,6	2,78	-2,24	0,707406 (0,000024)

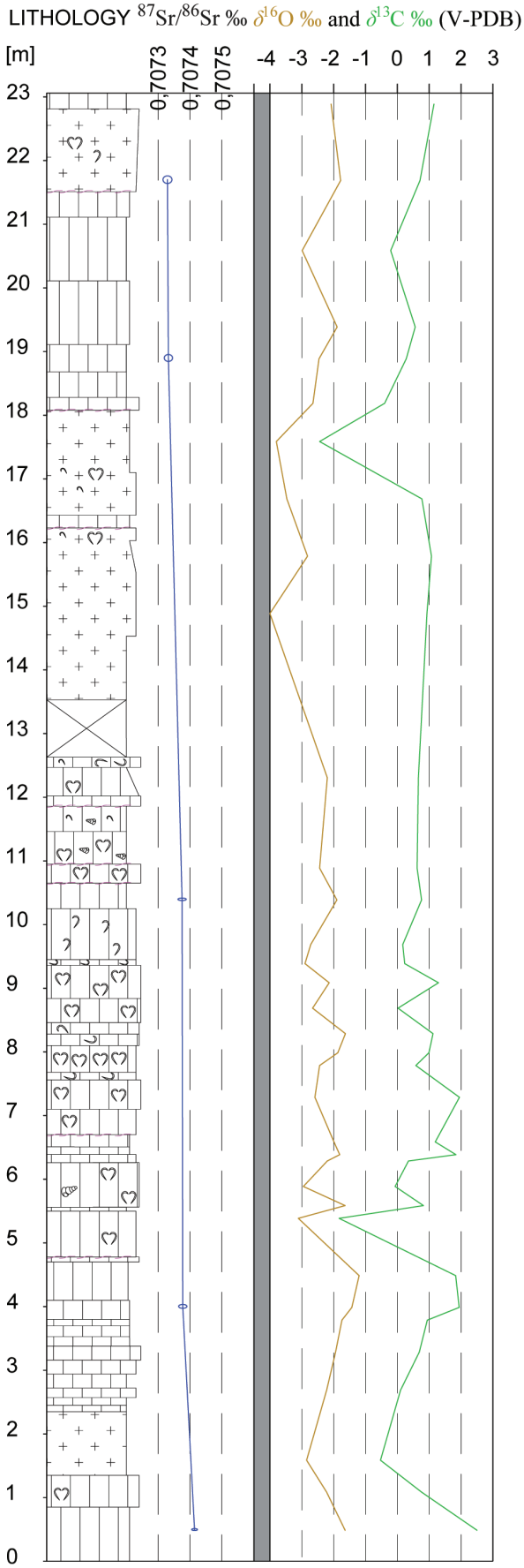

Fig. 10. $^{87}Sr/^{86}Sr$, $\delta^{13}C$ and $\delta^{18}O$ curves on a composite log with marked grains (see legend on Figure 4). Diameters of blue elipse represent the standard deviation of measurement (y axis) and the calculated local uncertainty (x axis) for the $^{87}Sr/^{86}Sr$ isotope values.

(r = 0.99), SiO_2 with K_2O (r = 0,98), and SiO_2 with TiO_2 (r = 0.99) are high. This is consistent with the data from the primary sedimentological section, with slightly higher correlations for the stone products due to the relatively small number of samples. The multi-method data obtained shows a direct match with the values obtained in the characterisation of the sedimentological sections in the antient Podpeč quarry; thus, the stone products can be assigned to their specific place of extraction. Based on Strontium isotopic values, the appropriate bed thickness and microfacies type, and the alignment with geochemical measurements the provenance of lorica NMS L210 can be placed in the lower part of the antient quarry (see Fig. 5 – probe 2), the studied inscriptions stones MGML 48572 and MGML 51180 in the upper part of the succession (see Fig. 5 – probe 3) and lorica NMS L209 to the upper most part of probe 3.

Discussion

Comparing the detailed geological map with the previous Basic Geological Map (Buser et al., 1967), new lithostratigraphic and structural relations could be interpretated from the detailed field data. On the western part of the St. Ana hill in the village of Podpeč, where lithostratigraphic division was in part recently presented (Djurić et al., 2018a), the new geological map shows good agreement with the geological boundaries and lithostratigraphic units presented therein. The new geological map defines the lithostratigraphic units available for quarrying on the wider Podpeč area (see Fig. 4a), and as seen from the digital elevation model (see Fig. 4b) all Members of the Lower Jurassic Podbukovje Formation have been quarried, either for the extraction of dimension stone (Djurić et al., 2018a; Djurić et al., 2022) and/or the production of lime (Bras, 1977).

None of the described facies is exclusive to the antique quarry, as all occur also within the younger part of the succession exposed in the modern quarry. The logged sedimentological sections record the lateral and vertical variability of microfacies typical for internally differentiated lagoonal sedimentation environments (Gale, 2015). The succession was previously placed in the Lithiotid Limestone Member (Djurič et al., 2022). However, based on the present sedimentological and paleontological data and the lack of lithiotid bivalves in the logged sections, this part could, alternatively, stratigraphically belong to the Orbitopsella Limestone Member. Knowing the detailed sedimentological composition of the beds within the antique quarry, however, it is much easier to locate the products back to the original place of extraction. Telling examples are the bivalve (mainly megalodontid bivalve) microfacies found only in the lower part of the antique quarry.

As no age-characteristic foraminifera for Pliensbachian could be found for the succession logged at the antient Podpeč quarry, foraminiferal assemblages can be used to suggest the stratigraphic position of this quarry. To some extent, the *Lituosepta recoarensis* lineage zone (Kabal & Tasli, 2003; Velić, 2007) can be considered as characteristic for the studied part of the succession. Additionally, individual microfacies show enough consistency to be considered one of the features that help to distinguish between different microfacies. The facies dependence of Early Jurassic benthic foraminifera has been hypothesised previously by Fugagnoli (2004) and attributed to gradients in trophic resources, oxygen levels, and stability in nutrient supply. As shown by Gale and Kelemen (2017), such differences among the assemblages can be recognized from the Sinemurian onwards. Most of the taxa from the investigated assemblages are considered to be benthic opportunists (see Fugagnoli, 2004). Most notably, these include *Meandrovoluta asiagoensis* and *Siphovalvulina*. On the other hand, *Haurania* represents a lituolid with a complex wall structure. The trophic levels would thus shift between eutrophic and mesotrophic conditions (Fugagnoli, 2004). Foraminifera assemblages of the beds within the antique quarry can help in provenance determinations of ancient stone products with the typical assemblages for microfacies described. Acquired geochemical data, both in primary samples and stone products, can be assigned to the carbonate and non-carbonate components. CaO, MgO, Sr, LOI, and partially also NaO were grouped to the carbonate component. The low MgO values indicate that the carbonate component belongs to low-Mg calcite, which was likely formed by early diagenetic processes from the high-Mg calcite and aragonite. Sr and Na_2O values are consistent with those measured in Lower Jurassic marine carbonates (Veizer et al., 1999; Hamon & Merzeraud, 2007; Ogorelec, 2009). The non-carbonate component includes AlO_3, K_2O, TiO_2, Zr, and most of the Na_2O, while SiO_2 can belong to the biogenic or terrigenous source. The high positive correlation of SiO_2 with Al_2O_3, K_2O and TiO_2 indicates that SiO_2 is also associated with a terrigenous influx. The low concentrations of non-carbonate components, specifically

the low values of K_2O, TiO_2, Al_2O_3, and Zr, show little terrigenous input, which is in accordance with sedimentation in a restricted lagoon of a carbonate platform (Buser & Debeljak, 1995; Debeljak & Buser, 1997; Gale, 2015). Some higher values of SiO_2 implies that the studied succession (and stone products originating from it) was occasionally under the influence of subaerial exposure (Martinuš, et al., 2012), which is again in accordance with previous studies (Gale, 2015). Non-carbonate components Fe_2O_3, MnO, and U are all interpretated as partially terrigenous and partially diagenetic. The very low values of MnO and Fe_2O_3 also indicate very low terrigenous and diagenetic influence, and the fact that the limestones were not enriched with minor and trace elements during the diagenetic processes and did not interact with circulating water of continental origin (Veizer, 1983). U values are higher in micritic and fine-grained limestones than they are in oolithic limestone, both in primary samples and in the studied stone products. We attribute this to a higher proportion of organic material in micritic samples (Goswami et al., 2017). Reported geochemical values herein can be considered, to some extent, typical for determinations of provenance in the ancient Podpeč quarry.

It must be kept in mind that in shallow marine environments terrigenous inputs can have a large influence on the isotopic record (Eystein, 1989), which means that local variations in isotope curves are possible. Previously defined low terrigenous input serves to strengthen the trust limit in the acquired data for the antient Podpeč quarry.

All studied samples show little to no effect of diagenetic changes, both in terms of the ratio of $\delta^{18}O$ and $\delta^{13}C$ isotopes (Table 2), as data points fall within values documented for Jurassic marine limestones (Veizer et al., 1999; Jenkyns et al. 2002; Hamon & Merzeraud, 2007). The widest range of carbon and oxygen values in micrite facies might be also due to the fact that they represent the largest data set in these microfacies. The measured ranges of isotopic ratios of carbon and oxygen overlap in most cases; thus, in the case of the ancient Podpeč quarry this method can be used for the determination of provenance only as one of the factors that strengthen the determination but cannot be considered decisive. Carbon and oxygen isotope measurements show alignment with ranges of values for each facies defined above, except for stone products made from oolithic facies, which in both stone products shows higher values. This is likely due to the small number of primary samples in these facies; thus, the full range of values was probably not detected.

The $^{87}Sr/^{86}Sr$ values of marine carbonates can be used for geochronological and correlative purposes by comparing them with global curves for a time-period of interest (McArthur et al., 2012a). If, based on microfacies and biostratigraphic analysis, the provenance of a specific stone product cannot be reliably determined, strontium isotope values can be used to derive a more exact provenance (Galan et al., 1999; Maritan et al., 2003; Brilli et al., 2010; Brilli et al., 2011). The measured range of strontium values can be considered characteristic for this part of the succession (Brajkovič et al., 2021) and thus used to define the provenance of ancient stone products (see Fig. 9c) and place the studied succession in the early Pliensbachian Orbitopsela Limestone Member (Orbitopsela Beds sensu Dozet & Strohmenger 2000).

The same stone products were studied in the publication by Djurić et al. (2022), where their origin could not be reliably determined based solely on petrological data. This is due to the frequent occurrence of micritic and fine-grained limestones in other putative quarry areas (Ramovš, 1990; Šašel Kos, 1997; Rožič et al., 2018). The presumed quarry areas of Podutik (Ramovš, 1990) and Staje (Šašel Kos, 1997) belong to the Krka Limestone Member (Novak, 2003; Rožič et al., 2018), where micritic and fine-grained facies are most abundant and oolithic facies are also present. The multi-method approach used enabled us to determine the exact provenance of these facies in studied stone products to the exact place of extraction in the antique Podpeč quarry.

Conclusions

Following the previous archaeological research, which located the Roman quarry at Podpeč (Djurić et al, 2022), the known extent of the antique quarry was studied in detail according to the multi-method approach.

A detailed lithological analysis of the beds quarried in the antique quarry revealed two facies assemblages that vary in the predominant facies component. From this, one of the transitions from a restricted to a more open marine lagoon was interpreted. The microfacies and expected foraminifera assemblages (see Tab. 1) provide a record of the antique quarry microfacies, which in turn lends more definitive credence to provenance determinations of the stone products to the Podpeč quarry. The low terrigenous influx and

the occasional sub-aerial exposure of the studied succession confirmed previous interpretations of the environment of sedimentation, and additionally provide values and correlations useful for provenance studies of the stone extracted from the ancient Podpeč quarry. The linear correlation of SiO_2 with Al_2O_3, K_2O, and TiO_2 is thus expected. This can serve as one of the factors when determining the origin of the stone; however, it cannot serve as the sole determining factor. Isotope values $\delta^{13}C$, $\delta^{18}O$, and $^{87}Sr/^{86}Sr$ can be considered typical for the antique quarry at Podpeč. Based on the lack of Lithiotid bivalves and the correlation of Sr isotopic values with the global record, the succession was lithostratigraphically correlated to the Orbitopsela Limestone Member (Orbitopsela beds sensu Dozet & Strohmenger, 2000). The $\delta^{13}C$ and $\delta^{18}O$ values cannot be considered decisive in determining origin from the Podpeč quarry; however, it can help in limiting the part of the succession from which the limestone was extracted. The Sr isotope measurements allow us to place the individual measurements of the stone products into the range typical for the ancient Podpeč quarry. Where the standard deviation of single measurements of stone product values is low, the Sr values compared with the logged facies (see Fig. 5) can enable us to place the stone product in the appropriate part of the succession.

For determination of the provenance of the stone used in Antiquity, it is recommended that a thin section be made for a detailed examination of the facies. For those microfacies that are distributed over the larger part of the Podbukovje Formation (micritic, fine-grained, and oolithic limestone), the reliable means of determining the provenience is the multi-method approach. Determining the provenance of stone products made from micritic, fine-grained, and oolithic microfacies, and the foraminifera assemblages described herein, combined with the geochemical and isotopic values provided in this paper, serve to provide a suitable reference for the stone material derived from the Podpeč quarry. This study additionally enables further detailed archaeological studies of the antique production and trade related to the Podpeč quarry.

Acknowledgements

This study was financially supported by the Slovenian Research Agency (Programme No. P1-0011 and No. P1-0025). We thank the reviewers for their valuable comments and suggestions that helped improve the manuscript. Additionally, we thank Mineral Ltd. and the Vehar family (Podpeč 44) for access to the premises; Dr. Ana Novak and Blaž Milanič for the preparation of digital elevation models and topographical data; Petra Škrap for help with the fieldwork; and Mladen Štumergar for the preparation of thin sections. For access to the museum collections and permissions for the sampling of stone products we thank Dr. Janka Istenič (National Museum of Slovenia) and Dr. Bernarda Županek (Museum of Ljubljana).

References

Brajkovič, R., Žvab Rožič, P. & Gale, L. 2021: Methodological approach to provenance determination of stone products made from micritic and fine-grained limestones. In: Rožič (ed.): Razprave, poročila = Treatises, reports: 25. posvetovanje slovenskih geologov = 25th Meeting of Slovenian Geologists. Univerza v Ljubljani, Naravoslovnotehniška fakulteta, Oddelek za geologijo, Ljubljana.

Bras, L. 1977: Apnenice v Podpeči pod Krimom. Slovenski etnograf, 30: 75-91.

Brilli, M., Antonelli, F., Giustini, F., Lazzarini, L. & Pensabene, P. 2010: Black limestones used in antiquity: the petrographic, isotopic and EPR database for provenance determination. Journal of Archaeological Science, 37/5: 994-1005. https://doi.org/10.1016/j.jas.2009.11.032

Brilli, M., Conti, L. Giustini, F., Occhiuzzi, M., Pensabene, P. & De Nuccio, M. 2011: Determining the provenance of black limestone artifacts using petrography, isotopes and EPR techniques: the case of the monument of Bocco. Journal of Archaeological Science, 38/6: 1377-1384. https://doi.org/10.1016/j.jas.2011.02.005

Brodar, S., Grafenauer, B., Klemenc, J., Korošec, J. & Rakovec, I. 1955: Zgodovina Ljubljane. Geologija in arheologija. DZS, Ljubljana: 458 p.

Buser, S., Grad, K. & Pleničar, M. 1967: Osnovna geološka karta SFRJ, list Postojna. Zvezni geološki zavod Jugoslavije, Beograd.

Buser, S. 1968: Osnovna geološka karta SFRJ, list Ribnica. Zvezni geološki zavod Jugoslavije, Beograd.

Buser, S. & Debeljak, I. 1995: Lower Jurassic beds with bivalves in South Slovenia. Geologija, 37/38: 23-62. https://doi.org/10.5474/geologija.1995.001

Debeljak, I. & Buser, S. 1997: Lithiotid Bivalves in Slovenia and Their Mode of Life. Geologija, 40/1, 11-64. https://doi.org/10.5474/geologija.1997.001

Dozet, S. & Strohmenger, C. 2000: Podbukovje Formation, Central Slovenia. Geologija, 43/2: 197-212. https://doi.org/10.5474/geologija.2000.014.

Dozet, S. 2009: Lower Jurassic carbonate succession between Predole and Mlačevo, Central Slovenia. RMZ-materials and geoenvironment, 56: 164-193.

Dunham, R.J. 1962: Classification of carbonate rocks according to depositional texture. In: Han, W.E. (eds.): Classification of carbonate rocks, A symposium Amer. Ass. Petrol. Geol Mem., 108–121. https://doi.org/10.1306/M1357

Djurić, B. & Rižnar, I. 2017: Kamen Emone / The rocks for Emona. In: Vičič, B. & Županek, B. (eds.): Emona MM: [urbanizacija prostora - nastanek mesta = urbanisation of space - beginning of a town]. Zavod za varstvo kulturne dediščine Slovenije: Mestni muzej, Muzej in galerije mesta Ljubljane: 121-144.

Djurić, B., Gale, L., Lozić, E., Kovačič, N. & Okršlar, Š. 2017: Podpeč pri Ljubljani - kamnolom, EŠD 12509; sondiranje. In: Stipančić, & Djurić, B. (eds.): Arheologija v letu 2017: dediščina za javnost: zbornik povzetkov: 14-15.

Djurić, B., Gale, L., Lozić, E. & Rižnar, I. 2018a: On the edge of the known. The quarry landscape at Podpeč. In: Janežič, M., Mulh, T., Nadbath, B. & Žižek, I. (eds.): Nova odkritja med Alpami in Črnim morjem. Rezultati raziskav rimskodobnih najdišč v obdobju med leti 2005 in 2015 = New Discoveries between the Alps and the Black Sea. Results from the roman sites in the period between 2005 and 2015, Zbornik 1. mednarodnega arheološkega simpozija / Proceedings of the 1st International Archaeological Conference, Ptuj, 8. in 9. oktober 2015 / Proceedings of the 1st International Archaeological Conference, Ptuj, 8th and 9th October 2015, Monografije CPA 6, 77-87.

Djurić, B., Gale, L. & Miletić, S. 2018b: Podpeč limestone for colonia Iulia Emona (Regio X. Venetia et Histria). In: Coquelet, C. et al. (eds.): Roman ornamental stones in Northwestern Europe: natural resources, manufacturing, supply, life & after-life: 107-112.

Djurić, B., Gale, L., Brajkovič, R., Bekljanov Zidanšek, I., Horn, B., Lozić, E., Mušič, B. & Vrabec, M. 2022: Kamnolom apnenca v Podpeči pri Ljubljani in njegovi izdelki. Arheološki Vestnik, 73: 155-198. https://doi.org/10.3986/AV.73.06

Embry, A. F. & Klovan, J.E. 1971: A Late Devonian Reef Tract on Northeastern Banks Island. Canadian Petroleum Geology, 19/4: 730-781.

Eystein, J. 1989: The use of stable oxygen and carbon isotope stratigraphy as a dating tool. Quaternary International, 1/1: 151-166. https://doi.org/10.1016/1040-6182(89)90013-X

Fugagnoli, A. 2004: Trophic regimes of benthic foraminiferal assemblages in Lower Jurassic shallow water carbonates from northeastern Italy (Calcari Grigi, Trento Platform, Venetia Prealps). Palaeogeogr., palaeoclimatol., palaeoecol., 205: 111-130. https://doi.org/10.1016/j.palaeo.2003.12.004

Galan, E., Carretero, M. I. & Mayoral, E. 1999: A methodology for locating the original quarries used for constructing historical buildings: application to Malaga Cathedral, Spain. Engineering Geology, 54/3-4: 287-298. https://doi.org/10.1016/S0013-7952(99)00042-3

Gale, L. 2015: Microfacies characteristics of the Lower Jurassic lithiotid limestone from Northern Adriatic Carbonate Platform Central Slovenia. Geologija, 58/2: 121-138. https://doi.org/10.5474/geologija.2015.010

Gale, L. & Kelemen, M. 2017: Early Jurassic foraminiferal assemlage in platform carbonates of Mt. Krim, central Slovenia. Geologija, 60/1: 99-115. https://doi.org/10.5474/geologija.2017.008.

Goswami, S., Bhagat, S., Zakaulla, S., Kumar, S. & Rai, A. K. 2017: Role of organic matter in uranium mineralisation in Vempalle dolostone; Cuddapah basin, India. Journal of the Geological Society of India, 89/2: 145-154. https://doi.org/10.1007/s12594-017-0578-y

Hamon, Y. & Merzeraud, G. 2007: C and O isotope stratigraphy in shallow-marine carbonate: a tool for sequence stratigraphy (example from the Lodève region, peritethian domain). Swiss Journal of Geosciences, 100/1: 71-84. https://doi.org/10.1007/s00015-007-1206-4

Jenkyns, H. C., Jones, C. E., Gröcke, D. R., Hesselbo, S. P. & Parkinson, D. N. 2002: Chemostratigraphy of the Jurassic System: applications, limitations, and implications for palaeoceanography. Journal of the Geological Society, 159/4: 351-378. https://doi.org/10.1144/0016-764901-130

Kabal, Y. & Tasli, K. 2003: Biostratigraphy of the Lower Jurassic carbonates from the Aydinick area (Central Taurides, S. Turkey) and morphological analysis of Lituolipora termieri (Hottinger, 1967). J. Foram. Res., 33: 338-351.

Kim, S.T., Mucci, A. & Taylor, B.E. 2007: Phosphoric acid fractionation factors for calcite and aragonite between 25 and 75 °C: Revisited. Chemical Geology, 246: 135-146. https://doi.org/10.1016/j.chemgeo.2007.08.005

Kramar, S., Bedjanič, M., Mirtič, B., Mladenovič, A., Rožič, B., Skaberne, D., Gutman, M.,

Zupančič, N. & Cooper, B. J. 2015: Podpeč limestone: a heritage stone from Slovenia. In: Pereira, D. et al. (eds.): Global heritage stone: towards international recognition of building and ornamental stones, London, 219-231. http://dx.doi.org/10.1144/SP407.2

Maritan, L., Mazzoli, C. & Melis, E. 2003: A multidisciplinary approach to the characterization of Roman gravestones from Aquilea (Udine, Italy). Archeometry, 45/3: 363-74. https://doi.org/10.1111/1475-4754.00114

Martinuš, M., Bucković, D. & Kukoć, D. 2012: Discontinuity surfaces recorded in shallow marine platform carbonates: an example from the Early Jurassic of the Velebit Mt. (Croatia). Facies, 58: 649-669. https://doi.org/10.1007/s10347-011-0288-7

McArthur, J. M., Howarth R. J. & Shields, G. A. 2012a: Strontium isotope stratigraphy. In: Gradstein, F. M, Ogg, J. G., Schmitz, M. D. & Ogg G.M. (eds): A Geologic Time Scale 2012, Elsevier B.V., 1: 127-144. https://doi.org/10.1016/C2011-1-08249-8

McArthur, J.M., Howarth, R.J. & Bailey, T.R. 2012b: Strontium Isotope Stratigraphy: LOWESS Version 3: Best Fit to the Marine Sr-Isotope Curve for 0–509 Ma and Accompanying Look-up Table for Deriving Numerical Age. The Journal of Geology, 109/2: 155-170. https://doi.org/10.1086/319243

Miler, M. & Pavšič, J. 2008: Triassic and Jurassic beds in Krim Mountain area (Slovenia). Geologija, 51/1: 87-99. https://doi.org/10.5474/geologija.2008.010

Miletić, S., Šmuc, A., Dolenec, M., Miler, M., Mladenovič, A., Gutman Levstik, M. & Dolenec, S. 2021: Identification and provenance determination of stone tesserae used in mosaics from Roman Celeia, Slovenia. Archaeometry, 64/3: 561-577. https://doi.org/10.1111/arcm.12742

Mirtič, B., Mladenovič, A., Ramovš, A., Senegačnik, A., Vesel, J. & Vižintin, N. 1999: Slovenski naravni kamen. Geološki zavod Slovenije, Zavod za gradbeništvo Slovenije, Naravoslovnotehniška fakulteta, Oddelek za geologijo, Ljubljana: 131 p.

Munsell color (Firm) 2010: Munsell rock color charts: with genuine Munsell color chips. MI: Munsell Color, Grand Rapids.

Müllner, A. 1879: Emona, archäologische Studien aus Krain. I.V. Kleinmayr & F. Bamberg, Laibach.

Novak, M. 2003: Upper Triassic and Lower Jurassic beds in the Podutik area near Ljubljana (Slovenia). Geologija, 46/1: 65-74. https://doi.org/10.5474/geologija.2003.004

Ogorelec, B. & Rothe, P. 1993: Mikrofazies, Diagenese und Geochemie des Dachsteinkalkes und Hauptdolomits in Süd-West-Slowenien = Mikrofacies, diageneza in geokemija dachsteinskega apnenca ter glavnega dolomita v jugozahodni Sloveniji. Geologija, 35: 81-181. https://doi.org/10.5474/geologija.1992.005

Ogorelec, B. 2009: Spodnje jurske plasti v Preserju pri Borovnici. Geologija, 52/1: 193-204. https://doi.org/10.5474/geologija.2009.019

Placer, L. 1999: Contribution to the macrotectonic subdivision of the border region between outhern Alps and External Dinarides. Geologija, 41: 223-255. https://doi.org/10.5474/geologija.1998.013

Ramovš, A. 1990: Gliničan od Emone do danes. Odsek za geologijo, VTOZD Montanistika, Fakulteta za naravoslovje in tehnologijo, Ljubljana: 171 p.

Ramovš, A. 2000: Podpeški in črni ter pisani lesnobrdski apnenec skozi čas. Mineral, Ljubljana: 115 p.

Romaniello, S.J., Field, M.P., Smith, H.B., Gordon, G.W., Kim, M.H. & Anbar, A.D. 2015: Fully automated chromatographic purification of Sr and Ca for isotopic analysis Journal of analytical atomic spectrometry, 30/9: 1906-1912. https://doi.org/10.1039/c5ja00205b.

Rosenbaum, J. & Sheppard, S.M. 1986: An isotopic study of siderites, dolomites and ankerites at high temperatures. Geochim. Cosmochim. Acta, 50/6: 1147-1150. https://doi.org/10.1016/0016-7037(86)90396-0

Rožič, B., Gale, L., Brajković, R., Popit, T. & Žvab Rožič, P. 2018: Lower Jurassic succession at the site of potential Roman quarry Staje near Ig (central Slovenia). Geologija, 61/1: 49-71. https://doi.org/10.5474/geologija.2018.004

Šašel Kos, M. 1997: The Roman Inscriptions in the National Museum of Slovenia / Lapidarij Narodnega muzeja Slovenije. Situla: razprave Narodnega muzeja Slovenije = dissertationes Musei nationalis Sloveniae, 35: 541 p.

Šmuc, A., Dolenec, M., Lesar-Kikelj, M., Lux, J., Pflaum, M., Šeme, B., Županek, B., Gale, L., Kramar, S. 2016: Variety of Black and White Limestone Tesserae Used in Ancient Mosaics in Slovenia. Archaeometry, 59/2: 205-221. https://doi.org/10.1111/arcm.12250

Veizer, J. 1983: Chemical diagenesis of carbonates: theory and application of trace element

technique. In: Arthur, M.A., Anderson, T.F., Kaplan, I.R., Veizer, J. & Land, L.S. (eds.): Stable Isotopes in Sedimentary Geology. Society of Economic Palaeontologists and Mineralogists, 3-100. https://doi.org/10.2110/scn.83.10

Veizer, J., Ala, D., Azmy, K., Bruckschen, P., Buhl, D., Bruhn, F., Carden, G.A.F., Diener, A., Ebneth, S., Godderis, Y., Jasper, T., Korte, C., Pawellek, F., Podlaha, O.G. & Strauss, H. 1999: 87Sr/86Sr, δ13C and δ18O evolution of Phanerozoic seawater. Chemical Geology, 161/1-3: 59-88. https://doi.org/10.1016/S0009-2541(99)00081-9

Velić, I. 2007: Stratigraphy and palaeobiogeography of Mesozoic benthic Foraminifera of the Karst Dinarides (SE Europe). Geologija Croatica, 60/1: 1-113.

Vlahović, I., Tišljar, J., Velić, I. & Matičec, D. 2005: Evolution of the Adriatic Carbonate Platform: Palaeogeography, main events, and depositional dynamics. Palaeogeography, Palaeoclimatology, Palaeoecology, 220/3-4: 333-360. https://doi.org/10.1016/j.palaeo.2005.01.011

Vodnik, P., Djurić, B. & Gale, L. 2017: Vrednotenje možnosti lokacije rimskega kamnoloma v Podutiku na podlagi sedimentološke analize. In: Rožič, B. (ed.): 23. posvetovanje slovenskih geologov = 23rd Meeting of Slovenian Geologists. Ljubljana, March 2017. Ljubljana: Univerza v Ljubljani, Naravoslovnotehniška fakulteta, Oddelek za geologijo.

Vrabec, M. & Fodor, L. 2006: Late Cenozoic tectonics of Slovenia: structural styles at the Northeastern corner of the Adriatic microplate. In: Pinter, N., Grenerczy, G., Weber, J., Stein, S. & Medek, D. (eds.): The Adria microplate: GPS geodesy, tectonics, and hazards. NATO Sei. Ser., IV, Earth Environ. Sei., 61: 151-168. https://doi.org/10.1007/1-4020-4235-3_10

Weis, D., Kieffer, B., Maerschalk, C., Barling, J., de Jong, J., Williams, G.A., Hanano, D., Pretorius, W., Mattielli, N., Scoates, J.S., Goolaerts, G., Friedman, R.M. & Mahony, J.B. 2006: High-precision isotopic characterization of USGS reference materials by TIMS and MC-ICP-MS. Geochemistry, Geophysics, Geosystems., 7/8: 1-30. https://doi.org/10.1029/2006GC001283

Wright, V.P. 1992: A revised classification of limestones. Sedimentary Geology, 76/3-4: 177–185. https://doi.org/10.1016/0037-0738(92)90082-3